Repurposing HSP70 Inducing Compounds for Targeting Post-Mitotic Cell Division: Novel Promises as Neuroprotectants

Renu Sharma and Pravir Kumar*

Molecular Neuroscience and Functional Genomics Laboratory, Delhi Technological University (Formerly DCE), Delhi, India

_____

ABSTRACT

The recent findings related to cell cycle re-entry mediated neurodegeneration in post mitotic neurons have triggered rampant research in this area. Cell cycle has been identified as a true, causative phenomenon occurring during prodromal stages of neurodegenerative diseases such as Alzheimer's disease and Parkinson's disease. Heat shock proteins are internal 'stress absorbing' machinery which comes into force to protect the cell against heat, oxidative stress. Owing to its chaperonic activity, HSP70 has been shown to mediate pro-survival pathways in several diseases including neurodegenerative diseases. We therefore set out to check whether HSP70 inducing compounds can be repurposed to target post-mitotic cell division. Various in silico methods such as homology modelling, Ramachandran plots, Lipinski filter, ADMET analysis and molecular docking studies were performed. We report novel potential of some HSP70 inducing compounds in ameliorating post-mitotic cell division led neurodegeneration which has wide implications in Alzheimer's disease and Parkinson's disease.

Keywords: Cell cycle; HSP70; Therapeutics; Neurodegeneration

_____

INTRODUCTION

Toxic protein burden has been identified as the common underlying molecular switch to neurodegeneration in several neurodegenerative diseases (NDD) such as Alzheimer's disease (AD), Parkinson's disease (PD), Huntington's disease (HD), Inclusion body myositis (IBM) and Poly myositis (PM). While a host of stressors which induce neuro-muscular degeneration (NMD) namely aging, oxidative stress, impaired ubiquitin proteasome system (UPS), mitochondrial breakdown, loss of function of protective proteins and mutations have been identified, the quest for new players has been on-going for the simple reason that the known players do not add up to all the outcomes of neurodegeneration. The ectopic re-entry of cell cycle in post-mitotic cells such as neurons and muscles has been recently identified as a culprit in NMD. Normally, the cell cycle remains suppressed for lifetime and these cells never divide. However, re-expression of cell cycle markers such as cyclin C, cyclin D, cyclin E along with other markers of active cell cycle has been observed in the AD, PD, ALS, PM and IBM. Moreover, the occurrence of cell cycle proteins during early stages of NDD and their co-existence with pathological proteins has placed fresh impetus on cell cycle re-entry (CCE) as a 'causal' phenomenon in NDD [1]. Once triggered, the cell cycle ensured DNA synthesis in S phase followed by severe neuronal death and neurodegeneration in various NDD [2]. The major thrust of present study is flavonoids which are a class of plant based phenolic compounds with high content in oranges, grapes, lemons, red wine and green tea. The signature properties of flavonoids include antioxidant, anti-inflammatory, anti-allergic, antiviral, antibacterial, anticancer, anti-hypertensive, insulin-sensitizing and anti-ischemic [3]. Moreover, flavonoids are well tolerated in human body and display enhanced bioavailability and negligible toxicity in comparison to their synthetic counter-parts. Furthermore, they have been shown to improve upon disease symptoms by modulating various signal transduction pathways. Molecular chaperones are a class of intracellular proteins which assist the misfolded/toxic protein in regaining its native conformation or alternatively mediating its degradation via UPS thus triaging protein homeostasis inside the cell. Heat shock proteins (HSPs) are molecular chaperones

_____

expressed constitutively in the nervous system which are involved in decreasing neurotoxicity and enhancing neuronal cell survival in various NDD [4,5]. HSP 70 has been shown to associate with p53and arrest the cell cycle at G_1/S. Further, the activity of cell cycle inhibitor p27 was modulated by HSP70 [6]. Furthermore, the G1/S transition markers cyclin D1 and E were reported to associate with elevated level of HSP70 in IBM and PM thereby speculating their strong co-relation [7]. Mounting evidence has outlined HSP70 induction as the major route in mediating pro-survival action of most drugs and biomolecules in PD and other NDD [8,9]. Moreover, we previously outlined Arimoclomol to be a promising neuroprotectant through HSP70 induction in cell cycle driven neurodegeneration [1,10]. Therefore, it is pertinent to understand that HSP70 inducing compounds could be a new line of neurotherapeutics in CCE mediated neurodegeneration. We carried out comprehensive data mining on HSP70 inducers in NDD and carried out the study with twenty compounds. Various virtual screening methods such as, Lipinski filter, Ghose and Veber parameters, pharmacophore generation and ADME analysis were applied to screen drug-like compounds. Further, Homology modelling, 3D structure validation and Ramachandran plots of proteins were performed to establish model accuracy. Finally, ligand-protein interactions were studied with the targets of interests; G_0/G_1 phase markers i.e. cyclin C and cyclin D1 through molecular docking studies. Our results have outlined strong potential of three HSP70 inducing compounds namely Indomethacin, Bimoclomol and Sesamol in attenuating levels of cyclin D1 and cyclin C. These observations may have promising implications in targeting CCE mediated neurodegeneration in AD, PD and HD. Our results have reinforced the promising potential of HSP70 inducers as novel neuroprotectants in ameliorating CCE mediated neurodegeneration.

MATERIALS AND METHODS

Data mining
Data mining was done with the keywords HSP70 inducing compounds in neurodegeneration in the NCBI database. Also, extensive literature survey was carried out. The filter criteria were set to HSP70 inducers in cell cycle and/or neurodegeneration and accordingly, list of 20 potential compounds was prepared.

Retrieval of ligand structure
The sdf files of all the 20 compounds were retrieved from the PubChem database (http://www.pubchem.ncbi.nlm.nih.gov/). The pubChem database stores physio-chemical and biological information of compounds from three different databases. Additionally, their structures, physical and chemical properties were also obtained.

Drug-likeliness analysis
The drug ability of all the 20 potential candidates was tested through Lipinski filter analysis via the online tool. As the name suggests, Lipinski's rule of five is used to distinguish between compounds which may be converted into drugs from the negative candidates of drug-likeliness. The five rules of Lipinski are: (a) molecular mass <500 Dalton, (b) logP < 5, (c) hydrogen bond donors< 5, (d) hydrogen bond acceptors< 10 and (e) Molar refractivity between 40 -130 [11]. The other two markers used for drug-likeness screening were Ghose filter and Veber rules (www.swissadme.ch/index.php). The qualifying parameters of Ghose filter are (a) molecular weight 160-480 (b) number of atoms 20-70 (c) molar refractivity 40-130 (d) molar refractivity -0.4-5.6 (e) polar surface area <140 [12]. Finally, the Veber rules of (a) rotatable bond count <=10 and (b) polar surface area <=140 were applied to the compounds [13].

ADMET analysis
The toxicity profiling of ligands was carried out through the online tool SwissADME (www.swissadme.ch/index.php). The Swiss ADME tool assessed the ligands on various parameters such as lipophilicity (logP), hydrophilic nature (logS) and Blood Brain Barrier (BBB) permeability.

Pharmacophore based target prediction
The pharmacophore is a spatial arrangement of electronic and steric properties of a ligand which are responsible for its biological response against a particular target. Pharmacophore based target prediction was done with web server PharmMapper(http://59.78.96.61/pharmmapper/index.php) [14].

Protein Homology modelling and Structural validation
The Brookhaven Protein Data Bank (PDB) was searched for suitable templates of cyclin D1 and cyclin C for homology modeling using the BLASTP search with default parameters. Accordingly, PDB ID 2W96.A and 3RGF for cyclin D1 and cyclin C respectively were selected. The homology modeling of given templates was performed using the Swiss Model server (http://swissmodel.expasy.org/) [15].

_____

The 3D model so generated was tested for structural and stereo-chemical evaluation using the online server RAMPAGE (http://www.mordred.bioc.cam.ac.uk/~rapper/rampage.php) [16]. The RAMPAGE tool allowed for residue by residue analysis of cyclin D1 and cyclin C geometry. Finally, the structural validation and accuracy of the models was checked with Errat(http://nihserver.mbi.ucla.edu/ERRATv2/).

Prediction of physio-chemical properties
The physio-chemical properties of cyclin D1 and cyclin C were predicted using the web based server ProtParam (http://web.expasy.org/protparam/) by using the Uniprot IDP24385 and P24863 respectively.

Active site prediction
The active sites of cyclin D1 and cyclin C were predicted using the Pock Drug tool(http://pockdrug.rpbs.univ-paris-diderot.fr/cgi-bin/index.py?page=home) [17]. The PDB structures of cyclin D1 and cyclin C were uploaded and binding pockets were predicted using the fpocket estimation and setting ligand proximity threshold at 5.5.

Preparation of proteins and ligands for docking
The proteins and ligands were prepared for docking using the online Docking Server (http://www.dockingserver.com/web) [18]. The proteins were cleaned and appropriate chain; A and B for cyclin D1 and cyclin C respectively selected for docking. Next, charge onprotein and ligands was added using Gasteiger method and solvation parameters set to default. The ligand geometry was optimized using MMFF94 method. Further, all non-polar H_2 atoms were merged, rotatable bonds defined and pH set to 7.0.

Molecular docking
The optimized proteins and ligands were used for molecular docking studies using the online Docking Server (http://www.dockingserver.com/web).The Autodock tool was used for adding Kollman united atom type charges, essential H_2 atoms and solvation parameters. Affinity grid maps were generated with 0.375 Å spacing [19]. Further, the van der Waals and electrostatic interactions were calculated using Autodock parameter set and distance-dependent dielectric functions respectively. Furthermore, the Lamarckian genetic algorithm and Soils and Wets local search method was used for docking simulations [20]. During docking, all rotatable torsions were dropped. Every docking study was arrived after ten different runs with a cut off energy estimation of 250000. Finally, translational step with 0.2Å, torsion and quaternion steps of 5 were used with a population size of 150.

<div align="center">

RESULTS

</div>

Selection of ligands
The compounds along with their structure, physical properties and signalling cascade modulated in NDD and neuro-oncology have been summarised in Table 1.

Screening for drug-likeness and ADMET Analysis of compounds
Most of the compounds passed drug-likeness parameters but failed ADMET analysis predictions (Table 2). Bimoclomol, Indomethacin and Sesamol qualified all the above parameters and were used in further study. While the bioavailability score of Sesamol and Bimoclomol was 0.55, Indomethacin had the highest predicted bioavailability of 0.56.
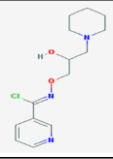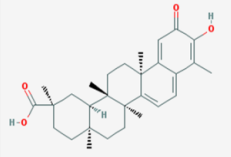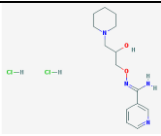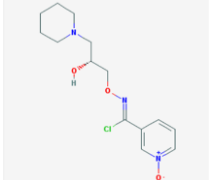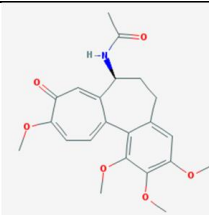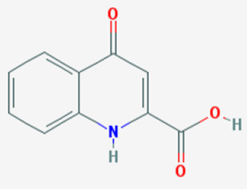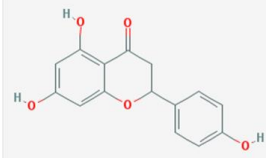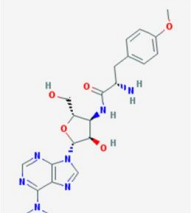
Pharmacophore based target prediction
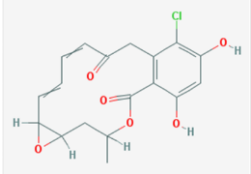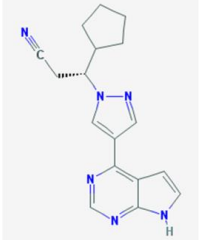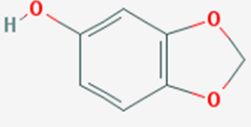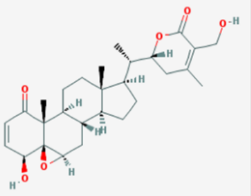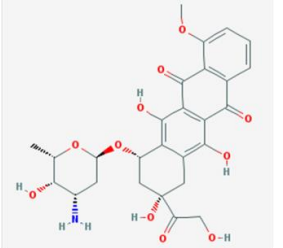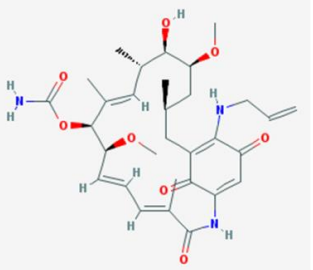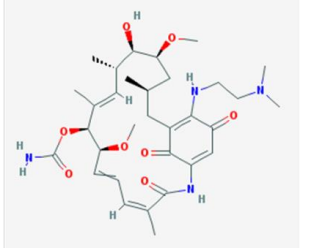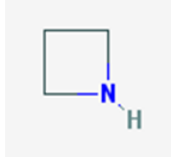The pharmacophore based target prediction of Indomethacin, Bimoclomol and Sesamol outlined various cell cycle proteins such as Cyclin A2, cell division protein kinase 2, VEGFR2 and MAPK18 which further strengthens our premise of their use in targeting cell cycle (Figure 1).

Homology modeling of proteins
The template shared 100% sequence similarity with cyclin D1 and cyclin C and was used to generate their 3D structures using Swiss Model. The Z QMEAN4 score indicative of overall quality of generated models with respect to non-redundant set of PDB structures was -1.68 and -0.64 for cyclin D1 and cyclin C respectively (Figure 2). Thus, the predicted protein structures satisfied good quality models.

R Sharma and P Kumar

J. Chem. Pharm. Res., 2017, 9(3):373-384

Table 1: Physio-chemical properties and modulated signalling pathways of compounds

S.No.	Compound	Structure	Molecular weight (g/mol)	Molecular formula	Modulated signalling in NDD/Neuro-oncology	References
1	Bimoclomol		297.783	$C_{14}H_{20}ClN_3O_2$	Augmented HSP70 level in ALS	[21]
2	Celastrol		450.619	$C_{29}H_{38}O_4$	Induced HSP70 and acted pro-survival in neurons post TBI damage, anti-inflammatory, Rapid induction of HSF1	[22]
3	BGP-15		351.272	$C_{14}H_{24}Cl_2N_4O_2$	Induced HSP70 and acted pro-survival in neurons post TBI damage, anti-inflammatory	[22]
4	Arimoclomol		313.782	$C_{14}H_{20}ClN_3O_3$	Induced HSP70, delayed progression of ALS	[21]
5	Colchicine		399.443	$C_{22}H_{25}NO_6$	Induced HSPB8 which in turn attenuated accumulation of misfolded TDP-43 and TDP-25 in ALS via HSP70/HSC70-CHIP complex	[23]
6	Indomethacin		357.79	$C_{19}H_{16}ClNO_4$	Induction of HSP70, attenuated Aβ induced damage in AD	[24]
7	Kyneuric Acid		189.17	$C_{10}H_7NO_3$	Inhibited proliferation, migration and DNA synthesis	[25]
8	Naringenin		272.256	$C_{15}H_{12}O_5$	Rescued against 6-OHDA induced toxicity through Nrf2/ARE signaling	[26]
9	puromycin		471.518	$C_{22}H_{29}N_7O_5$	Elicited HSP70 expression in response to ROS	[27]

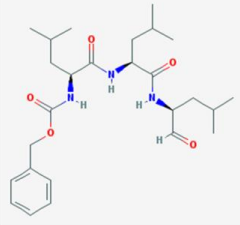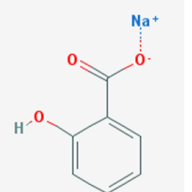| 10	Radicicol		364.778	$C_{18}H_{17}ClO_6$	Inhibit huntingtin aggresome, elevated HSP70	[28]
11	Ruxolitinib		306.373	$C_{17}H_{18}N_6$	Increased HSP70, Inhibited ERK1/2, Akt, STAT3 and STAT5	[29]
12	Sesamol		138.122	$C_7H_6O_3$	Protected against amyloidogenesis and cognitive dysfunction through NF-Kß inhibition	[30]
13	Withaferin		470.606	$C_{28}H_{38}O_6$	Induction of HSP70,HSP27,MAPK, Inhibition of Akt/Mtor and cell cycle at G2/M	[31]
14	Doxorubicin		543.525	$C_{27}H_{29}NO_{11}$	Induced HSPB8 which in turn attenuated accumulation of misfolded TDP-43 and TDP-25 in ALS via HSP70/HSC70-CHIP complex	[23]
15	17AAG		585.698	$C_{31}H_{43}N_3O_8$	Blocked cell proliferation through Wnt/β catenin pathway attenuation	[32]
16	17DMAG		616.756	$C_{32}H_{48}N_4O_8$	HSP70 induction, anti-inflammatory, anti-oxidant	[33]
17	Azitidine		57.096	C_3H_7N	protein synthesis inhibition, induction of chaperones	[34]
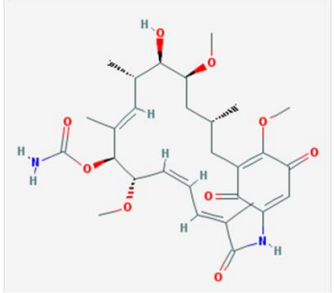
S.No	Compound	Structure	Mol. Wt.	Formula	Function	Ref
18	Geldanamycin		560.644	$C_{29}H_{40}N_2O_9$	Inhibit huntingtin aggresome, elevated molecular chaperones	[35]
19	MG132		475.63	$C_{26}H_{41}N_3O_5$	Induction of HSP70 in response to stress	[36]
20	Sodium Salicylate		160.104	$C_7H_5NaO_3$	Induction of HSP, imparting neuroprotection in rotenone induced PD	[37]

Table 2: Drug-likeness and ADMET screening analysis

S.No.	Compound	Drug likeness			Aq. Solubility		Lipophilicity	BBB	Bioavailability
		Lipinski	Ghose	Veber	LogS(ESOL)	GI permeability	XLogP3	Permeability	Score
1	Bimoclomol	Y	Y	Y	-2.9	High	2.21	Y	0.55
2	Celastrol	Y	N	Y	-6.31	Low	5.94	N	0.56
3	BGP-15	Y	Y	Y	-3.21	High	2.18	N	0.55
4	Arimoclomol	Y	Y	Y	-2.37	High	1.22	N	0.55
5	Colchicine	Y	Y	Y	-2.9	High	1.03	N	0.55
6	Indomethacin	Y	Y	Y	-4.86	High	4.27	Y	0.56
7	Kyneuric Acid	Y	Y	Y	-2.29	High	1.29	N	0.56
8	Naringenin	Y	Y	Y	-3.49	High	2.52	N	0.55
9	puromycin	Y	N	N	-2.51	Low	0.03	N	0.55
10	Radicicol	Y	Y	Y	-4.4	High	3.36	N	0.55
11	Ruxolitinib	Y	Y	Y	-3.26	High	2.12	N	0.55
12	Sesamol	Y	N	Y	-1.92	High	1.23	Y	0.55
13	Withaferin	Y	N	Y	-4.97	High	3.83	N	0.55
14	Doxorubicin	N	N	N	-3.91	Low	1.27	N	0.17
15	17AAG	Y	N	N	-4.67	Low	2.64	N	0.55
16	17DMAG	Y	N	N	-4.42	Low	2.04	N	0.55
17	Azitidine	Y	N	Y	-0.07	Low	-0.15	N	0.55
18	Geldanamycin	Y	N	N	-4.24	Low	1.99	N	0.11
19	MG132	Y	N	N	-4.77	High	4.83	N	0.55
20	Sodium Salicylate	Y	N	Y	-2.59	High	2.26	N	0.55

Quality assessment and physio-chemical description of 3D structures

The generated 3D structures were checked for validation in terms of steric and geometric conformations. For this, the Ramachandran plots were generated (Figure 2). The results showed 91.3% residues of cyclin D1 in the most favored region while 5.5% were in the allowed region. Further, 3.1% residues fell in outlier region. Similarly, for cyclin C 98.4% residues were seen in the favored region, 1.4% in the additionally allowed region and only 0.2% residues in the disallowed region. Further, cyclin D1 and cyclin C passed the model accuracy with 85.77% and 90.98% respectively. So overall, the structures of both the proteins were validated with good scores. The predicted physio-chemical properties of the models are summarized in Table 3.

_____

Ligand: 68289

	Rank	PDB ID	Target Name	Number of Feature	Fit Score	Normalized Fit Score	z'-score
+	8	3FZF	Heat shock cognate 71 kDa protein	6	2.899	0.4832	2.00718
+	9	1DYT	Eosinophil cationic protein	6	2.884	0.4806	1.62091
+	10	1HY7	Stromelysin-1	6	2.861	0.4769	0.716266
+	11	1TX4	Rho GTPase-activating protein 1	6	2.859	0.4765	1.56842
+	12	1DI8	Cell division protein kinase 2	6	2.819	0.4698	1.23631
+	13	1D3H	Dihydroorotate dehydrogenase, mitochondrial	6	2.765	0.4608	0.869469
+	14	1XO2	Cell division protein kinase 6	5	2.246	0.4492	-0.680011
+	15	1U4L	C-C motif chemokine 5	6	2.613	0.4354	0.630226
+	16	1H28	Cyclin-A2	6	2.606	0.4343	0.0851662

Ligand: 3715

	Rank	PDB ID	Target Name	Number of Feature	Fit Score	Normalized Fit Score	z'-score
+	1	3H9O	NONE	4	3.363	0.8409	0.519893
+	2	830C	Collagenase 3	4	3.22	0.805	-0.574694
+	3	2P2H	Vascular endothelial growth factor receptor 2	4	3.181	0.7952	-0.366195
+	4	2CLX	Cell division protein kinase 2	4	3.151	0.7877	-0.27883
+	5	3EID	Cell division protein kinase 2	5	3.828	0.7656	2.21778
+	15	1H28	Cyclin-A2	6	4.058	0.6764	2.52909

Ligand: 9576891

	Rank	PDB ID	Target Name	Number of Feature	Fit Score	Normalized Fit Score	z'-score
+	1	1ONG	Beta-lactamase SHV-1	4	3.548	0.8871	0.0454138
+	2	1DY4	Exoglucanase 1	4	3.525	0.8812	0.288696
+	3	1GCZ	Macrophage migration inhibitory factor	4	3.409	0.8523	-0.339281
+	4	2B55	Cell division protein kinase 2	5	3.802	0.7605	1.62195
+	5	2BTO	NONE	5	3.789	0.7578	1.49587
+	6	1Q6I	FKBP-type peptidyl-prolyl cis-trans isomerase fkpA	5	3.7	0.74	1.15025
+	7	3CPA	NONE	5	3.544	0.7087	-0.0490846
+	8	2ZAZ	Mitogen-activated protein kinase 14	5	3.521	0.7042	-0.408482

Figure 1: Pharmacophore based target prediction of Indomethacin, Sesamol and Bimoclomol (top to bottom in order)
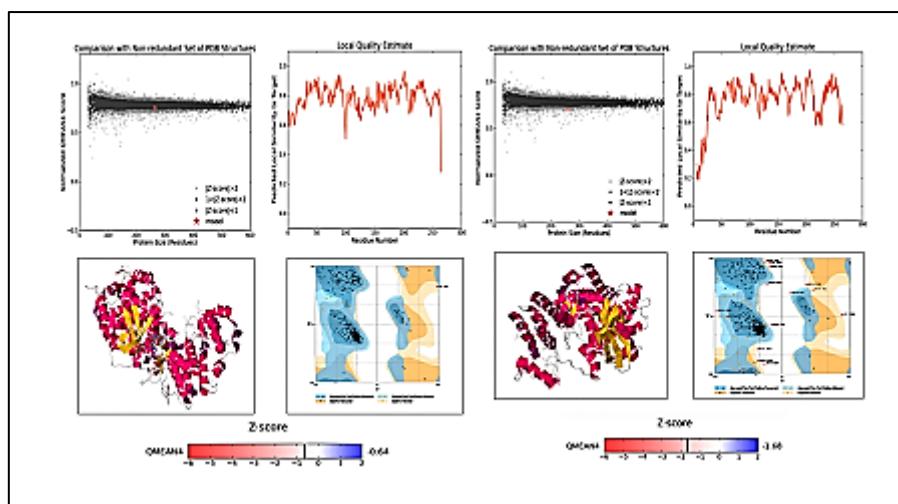
R Sharma and P Kumar

J. Chem. Pharm. Res., 2017, 9(3):373-384

_____

Figure 2: Structural validation of cyclin C and cyclin D1 (left to right)

Table 3: Predicted physio-chemical properties of cyclin D1 and cyclin C

Protein	Mol wt.	Atomic composition	No. of Amino Acids	Theoretical PI	Negatively charged residues Asp+Glu	Positively charged residues Arg+Lys	Instability index	Aliphatic index	GRAVY
Cyclin D1	33729.11	$C_{1480}H_{2386}N_{396}O_{450}S_{25}$	295	4.97	47	34	57.71	92.92	-0.185
Cyclin C	33242.73	$C_{1522}H_{2348}N_{384}O_{417}N_{17}$	283	6.95	32	32	49.97	92.69	-0.158

Active site prediction

Based on drugability score, cavity volume and standard deviation, cyclin D1 had best pocket at P5 with a score of 0.95 and 0.01 standard deviation (Figure 3a). The volume of given pocket was 1079.69 cubic angstroms and 16 residues were involved in interaction. Similarly, P0 was best predicted active site for cyclin C with 0.97 score (Figure 3b). The volume of this cavity was found to be 3732.64 cubic angstroms and 38 residues were involved in interaction at this site. These pockets were used for docking the ligands and same residues as predicted were found to be involved during docking.

Figure 3: Predicted active sites (top 10) in cyclin D1 (a) and cyclin C (b)

_____

Molecular docking of ligands with cyclin D1
Bimoclomol and cyclin D1: While the total intermolecular energy of Bimoclomol and cyclin D1 was -5.49kcal/mol, the estimated free energy of binding was found to be -4.77Kcal/mol (Figure 4a). Bimoclomol formed hydrogen bonds with LEU148 (-3.9537kcal/mol). Further, ASN151 was involved in polar bond formation with -1.0163kcal/mol and LEU91formed hydrophobic bond with Bimoclomol (44.6643kcal/mol).

 Indomethacin and cyclin D1: The estimated free energy of binding for cyclin D1-Indomethacin interaction was -5.51kcal/mol and total intermolecular energy was -6.68kcal/mol (Figure 4b). The H_2bond energy with ALA39 was unfavorable (23.1104kcal/mol). Further, two polar bonds were formed with ARG87 (-6.319kcal/mol) and SER41 (-2.497kcal/mol).

Sesamol and cyclin D1: Sesamol interacted with cyclin C to generate estimated free energy of binding -3.76kcal/mol and total intermolecular energy of -4.06kcal/mol. Polar bond was formed with ASN83 (-0.1798kcal/mol). Four hydrophobic bonds were formed with PRO199 (-0.9286kcal/mol), ALA39 (-0.5013kcal/mol), PRO40 (-0.2763kcal/mol) and PRO200 (-0.195kcal/mol) (Figure 4c).

Molecular docking of ligands with cyclin C
Bimoclomol and cyclin C: The estimated free energy of binding for cyclin C and Bimoclomol was -4.02kcal/mol, while the total intermolecular energy was -6.24kcal/mol. Hydrogen bond with -0.2489kcal/mol energy was formed between THR66. While the polar bond energy of ASP182 was -3.9173kcal/mol, hydrophobic bonds formed with TYR 184(-1.8162kcal/mol) and ILE62 (-0.3802kcal/mol). Further, GLN49 formed halogen bond with -7.6881kcal/mol energy (Figure 4d).

Indomethacin and cyclin C: Indomethacin interacted with cyclin C and generated high estimated binding energy of -5.68kcal/mol and total intermolecular energy -7.22kcal/mol. Further, five polar bonds were formed with ASN46, ARG185, GLN59, THR66 and GLN49 having energy values of -0.8421, -0.5951, -0.5475, -0.2608 and -0.2379 kcal/mol respectively. Next, two hydrophobic bonds were formed between TRP241 (-0.6165kcal/mol) and ILE62 (-0.4887kcal/mol) (Figure 4e).

Sesamol and cyclin C: The estimated free energy of binding for cyclin C-Bimoclomol interaction was -4.31kcal/mol and total intermolecular energy was -4.61kcal/mol. Two polar bonds were formed between TYR37 (-0.686kcal/mol) and ARG25 (-0.4014kcal/mol). Further, three hydrophobic bonds were formed with TYR73(-0.945kcal/mol), PHE69(-0.5898kcal/mol) and LEU78(-0.3605kcal/mol) (Figure 4f).
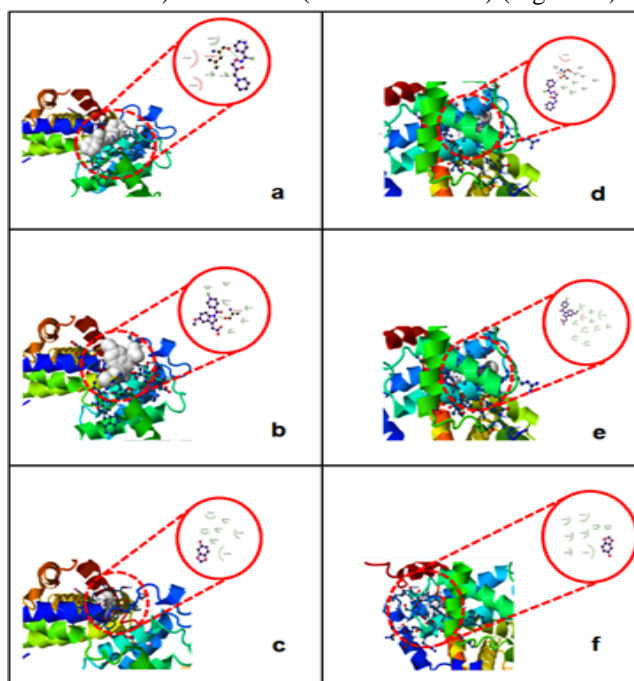

Figure 4: Docking of cyclin D1 with Bimoclomol, Indomethacin and Sesamol (a,b,c) and cyclin C (d,e,f) respectively with the interacting residues (inset)

_____

The comparative analysis of docking calculations was done (Table 4) and Indomethacin was found to be the best compound for targeting and inhibiting cyclin D1 as well as cyclin C thereby, implicating its strong and diverse potential in attenuating G_0/G_1 checkpoints in cell cycle.

Table 4: Comparative analysis of ligands-proteins docking calculations

Energy Parameters	CYCLIN D1			CYCLIN C		
	Bimoclomol	Indomethacin	Sesamol	Bimoclomol	Indomethacin	Sesamol
Estimated free energy of binding (Kcal/mol)	-4.77	-5.51	-3.76	-4.02	-5.68	-4.31
Estimated inhibition constant (uM)	317.57	91.17	1.74	1.12	69	696.84
vdW+Hbond+desolv energy (Kcal/mol)	-5.89	-6.67	-4.07	-6.11	-7.06	-4.6
Electrostatic energy (Kcal/mol)	0.41	-0.01	0.01	-0.13	-0.16	0
Total intermolecular energy (Kcal/mol)	-5.49	-6.68	-4.06	-6.24	-7.22	-4.61
Interacting surface	600.646	624.148	366.636	576.194	645.711	305.971

DISCUSSION

The cell cycle re-entry mediated neurodegeneration contributes heavily in the demise of post-mitotic neurons and muscles. Since cyclins C and D are first respondents of a re-activated cell cycle,thus, targeting these can be 'nib in the bud' strategy in halting/ameliorating the evil cascade of cell cycle led neuronal death. HSPs are molecular chaperones which are upregulated during stress to protect the cell against heat, hypoxia and ROS generation. HSP70 in particular, has been shown to promote neuronal cell survival by inducing autophagy and mediating the activation of pro-survival signaling cascades [4]. Moreover, HSP70 is closely associated with cell cycle and interacted with cyclin D1 in IBM and PM [7]. It is therefore imperative to search for compounds which can induce the level of HSP70 in NDD as a key neuroprotective strategy. Further, currently available drugs provide only symptomatic relief; therefore, flavonoids are favored by neuroscientists owing to their beneficial effects and negligible toxicity. In the present study, we proposed and tested the efficacy of HSP70 inducing compounds in ameliorating cell cycle led neurodegeneration in various NDD. Since most drugs fail on poor solubility, we screened the compounds for ADMET and pharmacokinetics analysis. It is evident that *in vivo* bioavailability of an orally administered drug is largely dependent on its aqueous solubility and dissolution in GI fluids [38]. More the water solubility and GI permeability, better the bioavailability. Similarly, lipophilicity of a drug affects various physiological properties such as the rate of metabolism, transport across cell membrane and interaction with binding sites of receptor. Further, drugs intended for CNS should have logP value less than four [39,40]. Indomethacin, Bimoclomol and Sesamol showed logP values of 4.27, 2.21 and 1.23 respectively.However, the most important property required of a compound to be a neuroprotective agent is the ability to cross Blood brain barrier (BBB). As expected, most compounds failed the BBB permeability parameter. Three biomolecules namely, Bimoclomol, Indomethacin and Sesamol could cross the BBB and combined with their high GI absoption, least violations of drug likeness and good bioavailability score, were the best candidates for targeting NDD in our study. Further, pharmacophore based target prediction of these three compounds listed various cell cycle proteins which further supported our repurposing premise. Finally, molecular docking studies indicated Indomethacin as the best compound for HSP70 mediated targeting of post-mitotic cell cycle based on its high pharmacokinetics and docking calculations. Further, our results are backed by various *in vitro* and *in vivo* studies wherein these compounds have displayed promising neuroprotective action in various NDD. For instance, Bimoclomol has its derivative Arimoclomol already under Phase II clinical trials in ALS [41]. Indomethacin was shown to ameliorate Aβ1-42 triggered damage in AD mice model as well as in hippocampal cultures [24]. Similarly, Sesamol reversed PD linked symptoms in a rotenone model [42]. Hence, our compounds are validated for their neuroprotective action and yet, add to the hunt for protective biomolecules in alleviating cell cycle led neurodegeneration.Our study has outlined novel potential of Indomethacin, Bimoclomol and Sesamol in inhibiting/down-regulating the level of cyclin D1 and cyclin C. Out of these, Indomethacin showed best binding with both the cyclins, speculating its strong potential in inhibiting G_0/G_1 phase reactivation in terminally differentiated neurons in various NDD. Further, the protective action of these compounds in attenuating cell cycle re-entry may be mediated through HSP70. These findings can open up a new window of therapeutics for targeting ectopic cell cycle activation led neurodegeneration and need further validation through *in vitro* and *in vivo* cell cycle studies.

CONCLUSION

The study evaluated the potential of HSP70 inducing compounds for targeting post-mitotic cell cycle in neurodegenerative disorders. Based on BBB permeability, pharmacokinetic properties and ADMET analysis, we have shortlisted Indomethacin, Bimoclomol and Sesamol amongst twenty compounds for targeting cell cycle proteins; cyclin D1 and cyclin C. Further, our study demonstrated that Indomethacin has the highest potential in stalling or inhibiting cell cycle, based on high free energy of binding with both the markers of G_0/G_1 phase.

_____

Moreover, the cell cycle inhibiting effect of these compounds may be elicited through HSP70 induction. To the best of our knowledge, these compounds are novel for their use in targeting post mitotic cell division in neurodegenerative disorders

ACKNOWLEDGEMENT

REFERENCES

[1]   R Sharma; D Kumar; NK Jha; SK Jha; RK Ambasta; P Kumar. *Biochim Biophys Acta,* **2017**, 1863(1), 324-336.
[2]   K Herrup. *Alzheimers Res Ther,* **2010**, 2(3), 13.
[3]   D Procházková; I Boušová; N Wilhelmová. *Fitoterapia,* **2011**, 82, 513–523.
[4]   PJ Muchowsk; JL Walker. *Nat Rev Neurosci* , **2005**, 6, 11–22.
[5]   J Magrane; RC Smith; K Walsh; HW Querfurth. *J Neurosci*, **2004**, 24, 1700-1706.
[6]   J Liu; D Zhang; X Mi; Q Xia; Y Yu; Z Zuo; W Guo; X Zhao; J Cao; Q Yang; A Zhu; W Yang; X Shi; J Li; C Huang. *J Biol Chem*, **2010**, 285(34), 26058-26065.
[7]   B Kwon; P Kumar; HK Lee; L Zeng; K Walsh; Q Fu. *Hum Mol Genet*, **2014**, 23, 3681–3694.
[8]   XQ Bao; XL Wang; D Zhang. *Mol Neurobiol*, **2017**, 54 (1), 349-361.
[9]   CA Deane; IR Brown. *Cell Stress Chaperon*, **2016**, 21(5), 837-48.
[10]   DA Parfitt; M Aguila; CH McCulley; D Bevilacqua; HF Mendes; D Athanasiou; SS Novoselov; N Kanuga; PM Munro; PJ Coffey; B Kalmar. *J Neurochem*, **2008**, 107, 339-350.
[11]   CA Lipinski; F Lombardo; BW Dominy; PJ Feeney. *Adv Drug Deliv Rev*, **2001**, 46 (1-3), 3-26.
[12]   AK Ghose; VN Viswanadhan; JJ Wendoloski. *J Com Chem*, **1999**, 1, 55-68.
[13]   DF Veber; SR Johnson; HY Cheng; BR Smith; KW Ward; KD Kopple. *J Med Chem*, **2002**, 45 (12), 2615-2623.
[14]   L Xiaofeng; O Sisheng; Y Biao; H Kai; L Yabo; G Jiayu; Z Sisuan; L Zhihua; L Honglin; J Hualiang. *Nucleic Acid Res*, **2010**, 38, W609-W614.
[15]   M Biasini; S Bienert; A Waterhouse; K Arnold; G Studer; T Schmidt; F Kiefer; TG Cassarino; M Bertoni; L Bordoli; T Schwede. *Nucleic Acids Res*, **2014**, 42(W1), W252-W258
[16]   SC Lovell; IW Davis; WB 3rd Arendall; PI de Bakker; JM Word; MG Prisant; JS Richardson; DC Richardson. *Proteins*, **2003**, 50(3), 437-50.
[17]   HA Hussein; A Borrel; C Geneix; M Petitjean; L Regad; A Camproux. *Nucl Acids Res*, **2015**.
[18]   Z Bikadi; E Hazai. *J Cheminf*, **2009**, 1, 15.
[19]   GM Morris; DS Goodsell. *J Computational Chem*, **1998**, 19(14), 1639-1662.
[20]   FJ Soils; RJB Wets. *Mathematics of Operations Research*, **1981**, 6(1), 19-30.
[21]   SC Benn; RH Jr Brown. *Nat Med*, **2004**, 10(4), 345-7.
[22]   B Eroglu; DE Kimbler; J Pang; J Choi; D Moskophidis; N Yanasak; KM Dhandapani; NF Mivechi. *J Neurochem*, **2014**, 130(5), 626-41.
[23]   V Crippa; VG D'Agostino; R Cristofani; P Rusmini; ME Cicardi; E Messi; R Loffredo; M Pancher; M Piccolella; M Galbiati; M Meroni; C Cereda; S Carra; A Provenzani; A Poletti. *Sci Rep*, **2016**, 6, 22827.
[24]   A Bernardi; RL Frozza; A Meneghetti; JB Hoppe; AM Battastini; AR Pohlmann; SS Guterres; CG Salbego. *Int J Nanomedicine*, **2012**, 7, 4927-4942.
[25]   K Walczak; S Deneka-Hannemann; B Jarosz; W Zgrajka; F Stoma; T Trojanowski; WA Turski; W Rzeski. *Pharmacol Rep*, **2014**, 66(1), 130-136.
[26]   H Lou; X Jing; X Wei; H Shi; D Ren; X Zhang. *Neuropharmacol*, **2014**, 79, 380-388.
[27]   DM Moran; H Shen; CG Maki. *BMC Cell Biol*, **2009**, 10, 32.
[28]   DG Hay; K Sathasivam; S Tobaben; B Stahl; M Marber; R Mestril; A Mahal; DL Smith; B Woodman; GP Bates. *Hum Mol Genet*, **2004**, 13(13), 1389-1405.
[29]   M Tavallai; L Booth; JL Roberts; A Poklepovic P Dent. *Front Oncol*, **2016**, 6,142.
[30]   Z Liu; Y Chen; Q Qiao; Y Sun; Q Liu; B Ren; X Liu. *MolNutr Food Res*, **2016**.
[31]   PT Grogan; KD Sleder; AK Samadi; H Zhang; BN Timmermann; MS Cohen. *Invest New Drugs*, **2013**, 31(3), 545-557.
[32]   KK Chen; ZM He; BH Ding; Y Chen; LJ Zhang; L Yu; J Gao. *Zhongguo Shi Yan Xue Ye XueZaZhi*, **2016**, 24(1), 117-121.

_____

[33]   YL Wang; HH Shen; PY Cheng; YJ Chu; HR Hwang; KK Lam; YM Lee. *PLoS One*, **2016**, 11(5), e0155583.

[34]   CP Reina; BY Nabet; PD Young; RN Pittman. *Cell Stress Chaperon*, **2012**, 17(6), 729-742.

[35]   A Sittler; R Lurz; G Lueder; J Priller; H Lehrach; MK Hayer-Hartl; FU Hartl; EE Wanker. *Hum Mol Genet*, **2001**, 10(12), 1307-1315.

[36]   CI Holmberg; SA Illman; M Kallio; A Mikhailov; L Sistonen. *Cell Stress Chaperon*, **2000**, 5(3), 219-228.

[37]   P Thakur; B Nehru. *Neurochem Int*, **2014**, 75, 1-10.

[38]   P Khadka; R Jieun; H Kim; I Kim; JT Kim; H Kim; G Yun; J Lee. *Asian J Pharm Sci*, **2014**, 9(6), 304-316.

[39]   LK Chico; LJ Van Eldik; DM Watterson. *Nat Rev Drug Discov*, **2009**, 8(11), 892-909.

[40]   TT Wager; X Hou; PR Verhoest; A Villalobos. *ACS ChemNeurosci*, **2010**, 1(6), 435-449.

[41]   JM Keppel Hesselink. *J Pain Relief*, **2016**, 6, 279.

[42]   SM Angeline; A Sarkar; K Anand; RK Ambasta; P Kumar. *Neurosci*, **2013**, 254, 379-394.